# Eulerian and Lagrangian statistics in an exactly solvable turbulent shear model with a random background mean

Mustafa A. Mohamad and Andrew J. Majda
*Courant Institute of Mathematical Sciences, New York University*

July 1, 2019

**Abstract**

We study the Lagrangian statistics of passively advected particles in an elementary velocity model for turbulent shear. The stochastic velocity model is exactly solvable and includes features that highlight the important differences between Lagrangian and Eulerian velocity statistics, which are not equal in the present context. A major element of the velocity model is the presence of a random, spatially uniform background mean, which is superimposed on a turbulent shear with a spectrum that typically follows a power law. We directly solve for the Eulerian and Lagrangian statistics, and show how the sweeping motion of the background mean affects the Lagrangian velocity statistics with faster decaying correlations that oscillate more rapidly compared to the Eulerian velocity. This stems from an important interplay between the sweeping component from the mean and the shear component that determines tracer transport characteristics. We derive explicit expressions for the tracer dispersion that demonstrate how the mixing rate depends on model parameters. We validate the predictions with numerical experiments in various test regimes that also highlight the behavior of Lagrangian particles in space. The proposed model serves as an important test case for Eulerian spectral recovery via Lagrangian data assimilation and parameter estimation.

**Contents**

## 1 Introduction

We study the statistics of Lagrangian tracers or drifters advected by turbulent stochastic velocity fields. Lagrangian drifters are massless particles that are passively advected throughout a flow field and serve as an important data collection source for atmospheric and oceanographic measurements [1, 2]. Lagrangian models are commonly used to model pollution transport and air quality [3], turbulent combustion [4, 5], turbulent entrainment processes [6], particle aggregation, and turbulence [7, 8] due to the conceptual simplicity of the viewpoint and its connection with the physics of mixing and dispersion [9]. A key problem for any Lagrangian model is to understand the affects of the flow field on the statistical (ensemble) properties of the particles.

We propose here an elementary turbulent velocity model, consisting of a random shear and a random spatially uniform mean. The velocity model is exactly solvable, and is used to highlight the differences between Eulerian and Lagrangian velocity statistics, which are not equivalent in the current context. We derive explicit equations for the Eulerian and Lagrangian velocity correlation functions and the second-order moment of the drifters in the short and long time limits. We demonstrate how various features of the model interact to determine particle behavior. In particular, we discuss the important interplay between the mean and the shear component of the velocity model in determining tracer transport and mixing properties. We explicitly show how *the sweeping motion of the background mean affects the Lagrangian velocity statistics with faster decaying correlations that oscillate more rapidly compared to the Eulerian velocity.* This fact has significant implications in the spectral recovery problem, since the Fourier transform of the velocity correlation gives the kinetic energy spectrum [10]. There is a rich range of model regimes that determine particle behavior and mixing rates, which we explain and demonstrate by appealing to both numerical simulations and theory.

The Lagrangian characterization of diffusion processes and their statistics have been studied in various contexts over the years. The seminal paper by Taylor [11] studied diffusion due to the continuous motion of particles. The characterization and modeling of both single particle and multiple particle (pairs or groups) statistics, including data from observations, was later expanded upon and summarized in important works by Batchelor [12, 13], Richardson [14], and others in [15–20]. The statistical characterization of Lagrangian motions is crucial since Lagrangian instruments are a dominant data collection method in studying the atmosphere and ocean, since they can cover large distances and regions compared to costly fixed Eulerian measurement devices [1]. In recent studies, Lagrangian observational data from surface drifters and floats in the ocean have been used to study various properties of the ocean including, e.g., the kinetic energy spectrum and pair dispersion statistics in the Gulf of Mexico [21, 22] and to construct eddy diffusivity approximations of the global map [23].

Complementary to the Lagrangian viewpoint, the Eulerian characterization and study of turbulent diffusion and mixing has its own significance [24–26]. The report [26] studied simple mathematical models for turbulent diffusion of passive scalar fields, which connect and explain anomalous diffusion in random velocity field models. The Eulerian approach studying passive scalar statistics for a random shear flow with a mean sweep has been carried out in different context in [27–30]. Despite the simplicity of such problems, they capture and preserve key features in various inertial range statistics for turbulent diffusion, including intermittency and extreme events [27, 31] and serve as important paradigm models.

Our approach studies the Lagrangian statistics of a random shear model with a random background mean. We remark that the model has a special conditionally Gaussian structure [32, 33] (conditional on observed trajectories). Despite a conditional Gaussian velocity field, the tracer statistics remain nonlinear and non-Gaussian, since the Lagrangian observations are coupled nonlinearly to the velocity field. The exactly solvable nature of the proposed model makes it suitable as benchmark problem for Lagrangian data assimilation and parameter estimation [34–38], including the spectral recovery of the turbulent Eulerian velocity field and uncertainty quantification [39]. Filtering such conditionally Gaussian models for Lagrangian data assimilation have been explored in [40–42]; in particular [41, 42] develop mathematical guidelines and information theoretical limits on recovery and in [40] the spectral recovery performance and filter approximations are studied. The intuition and regime studies we conduct on the shear model provides guidelines for further studies on the estimation and spectral recovery problem, and can help interpreting when spectral recovery is an attainable goal and when recovery performance is expected to be poor, in the Lagrangian data assimilation problem.

### 1.1 Outline

In section 2, we provide an overview of Lagrangian and Eulerian statistics. The general velocity model is described in section 3, and the aligned shear test model in section 4. The Eulerian statistics for the aligned shear model are discussed in section 5. The Lagrangian statistics, including the mean Lagrangian velocity and Lagrangian velocity fluctuations, are then derived in section 6; the final result for the Lagrangian correlation is given in section 6.4. We discuss the differences between the Eulerian and Lagrangian velocity correlation functions in section 6.4. In section 8, we derive results for the mixing rate in various regimes and discuss the mixing properties in terms of model parameters. Numerical simulations and regime studies are presented in section 9. Concluding remarks are made in section 10.

## 2 Overview on Lagrangian and Eulerian statistics

We describe some elementary facts regarding Eulerian and Lagrangian velocity fields and the motion of tracer particles under fluid flows. The Eulerian velocity field is described in terms of a fixed system of space-time coordinates $\boldsymbol{v}(\boldsymbol{x}, t)$, which denotes the velocity of a fluid at position $\boldsymbol{x}$ and time $t$. In the Lagrangian description, we mark or label particles at time zero by their initial spatial coordinate $\boldsymbol{\alpha}$. The position at later times of the particle trajectory labeled $\boldsymbol{\alpha}$ is described by the function $\boldsymbol{X}(\boldsymbol{\alpha}, t)$ that satisfies

$$\frac{d\boldsymbol{X}(\boldsymbol{\alpha}, t)}{dt} = \boldsymbol{v}(\boldsymbol{X}(\boldsymbol{\alpha}, t), t), \qquad \boldsymbol{X}(\boldsymbol{\alpha}, 0) = \boldsymbol{\alpha}. \tag{1}$$

The Lagrangian velocity is defined by the velocity of the particle labeled by $\boldsymbol{\alpha}$ at time $t$, and is related to the Eulerian velocity field as follows,

$$\boldsymbol{v}^{\mathsf{L}}(\boldsymbol{\alpha}, t) \equiv \boldsymbol{v}(\boldsymbol{X}(\boldsymbol{\alpha}, t), t). \tag{2}$$

In principle, if the Lagrangian velocity field is known, we can directly obtain the particle trajectories by

$$\boldsymbol{X}(\boldsymbol{\alpha}, t) = \boldsymbol{\alpha} + \int_0^t \boldsymbol{v}^{\mathsf{L}}(\boldsymbol{\alpha}, s)\, ds. \tag{3}$$

However, this is usually not possible since determining the Lagrangian velocity from the Eulerian velocity, itself requires knowledge of tracer particle trajectories.

### 2.1 Eulerian and Lagrangian statistics

In general, we consider velocity models with a mean, so we separate the randomly fluctuating component of the Eulerian and Lagrangian velocities from their statistical mean, $\boldsymbol{v} = \overline{\boldsymbol{v}} + \widetilde{\boldsymbol{v}}$, where $\overline{\boldsymbol{v}} = \langle \boldsymbol{v} \rangle$, and similarly for the Lagrangian velocity $\boldsymbol{v}^{\mathsf{L}} = \overline{\boldsymbol{v}}^{\mathsf{L}} + \widetilde{\boldsymbol{v}}^{\mathsf{L}}$, where $\overline{\boldsymbol{v}}^{\mathsf{L}} = \langle \boldsymbol{v}^{\mathsf{L}} \rangle$.

We define some important statistical quantities of interest. The Eulerian velocity correlation function is defined by

$$R(\boldsymbol{x}_1, \boldsymbol{x}_2, t_1, t_2) = \langle \widetilde{\boldsymbol{v}}(\boldsymbol{x}_1, t_1) \widetilde{\boldsymbol{v}}(\boldsymbol{x}_2, t_2)^* \rangle. \tag{4}$$

The Lagrangian velocity correlation function of particle drifter pairs is given by

$$R^{\mathsf{L}_2}(\boldsymbol{x}_1, \boldsymbol{x}_2, t_1, t_2) = \langle \widetilde{\boldsymbol{v}}^{\mathsf{L}}(\boldsymbol{x}_1, t_1) \widetilde{\boldsymbol{v}}^{\mathsf{L}}(\boldsymbol{x}_2, t_2)^* \rangle, \tag{5}$$

and the Lagrangian autocorrelation function of a single drifter by

$$R^{\mathsf{L}}(\boldsymbol{\alpha}, t_1, t_2) = R^{\mathsf{L}_2}(\boldsymbol{\alpha}, \boldsymbol{\alpha}, t_1, t_2) = \langle \widetilde{\boldsymbol{v}}^{\mathsf{L}}(\boldsymbol{\alpha}, t_1) \widetilde{\boldsymbol{v}}^{\mathsf{L}}(\boldsymbol{\alpha}, t_2)^* \rangle. \tag{6}$$

Knowledge of the Lagrangian velocity correlation function fully describes the statistical correlations between positions of particle pairs moving throughout the flow. The Lagrangian autocorrelation function, fully describes the second order moment of a single particle in time. In general, Eulerian and Lagrangian statistics are not equivalent, since $\boldsymbol{v}$ and $\boldsymbol{v}^{\mathsf{L}}$ are not equal for most non-trivial flow fields.

When the statistics of the velocity field are homogeneous and stationary, the correlations depend only on the separation of spatial positions and time. This means that the correlation function is invariant under spatial and temporal translations: $R(\boldsymbol{x}_1, \boldsymbol{x}_1 + \boldsymbol{x}, t_1, t_1 + t) = R(\boldsymbol{x}, t)$. For random fields that are homogeneous and stationary, the mean must be constant and thus at a minimum, the structure of the field is contained in the correlation function.

The mean tracer displacement and the tracer's fluctuations about the mean are given by, respectively,

$$\overline{\boldsymbol{X}}(\boldsymbol{\alpha},t) = \langle \boldsymbol{X} \rangle = \boldsymbol{\alpha} + \int_0^t \overline{\boldsymbol{v}}^{\mathsf{L}}(\boldsymbol{\alpha},s)\,ds, \quad \widetilde{\boldsymbol{X}}(\boldsymbol{\alpha},t) = \boldsymbol{X} - \langle \boldsymbol{X} \rangle = \int_0^t \widetilde{\boldsymbol{v}}^{\mathsf{L}}(\boldsymbol{\alpha},s)\,ds. \tag{7}$$

The tracer variance can then be shown to be given by

$$\sigma^2_{\boldsymbol{X}}(t) = \langle \widetilde{\boldsymbol{X}}(\boldsymbol{\alpha},t)\widetilde{\boldsymbol{X}}(\boldsymbol{\alpha},t)^* \rangle = \int_0^t \int_0^t R^{\mathsf{L}}(\boldsymbol{\alpha},s,s')\,ds\,ds' = 2\int_0^t (t-\tau) R^{\mathsf{L}}(\boldsymbol{\alpha},\tau)\,d\tau, \tag{8}$$

where the last equality holds if the autocorrelation function is stationary, and can be shown using a change of variables.

## 3 A general random turbulent shear velocity model with a random spatial mean

We consider a two-dimensional random shear velocity model on a periodic domain given by,

$$\boldsymbol{v}(\boldsymbol{x},t) = \boldsymbol{w}(t) + \boldsymbol{u}(\boldsymbol{x},t) = \boldsymbol{w}(t) + \sum_{1\le|k|\le\Lambda} a_{\boldsymbol{k}}(t)\frac{i\boldsymbol{k}^{\perp}}{k} e^{i\boldsymbol{k}\cdot\boldsymbol{x}}, \quad a^*_{-\boldsymbol{k}} = a_{\boldsymbol{k}}, \tag{9}$$

on a total grid of $N = (2\Lambda+1)^2$ points, consisting of a spatially uniform mean $\boldsymbol{w}$ and shear $\boldsymbol{u}$. The dynamics of the background mean $\boldsymbol{w}$ and the Fourier coefficients $a_{\boldsymbol{k}}$, representing fluctuations relative to the background mean, are given by, respectively,

$$d\boldsymbol{w}(t) = \big((-\Gamma_0 + \Omega_0)\boldsymbol{w}(t) + \boldsymbol{f}_0\big)\,dt + \Sigma_0\,d\boldsymbol{W}_0(t), \tag{10}$$

$$da_{\boldsymbol{k}}(t) = \big((-d_{\boldsymbol{k}} + i\omega_{\boldsymbol{k}})a_{\boldsymbol{k}}(t) + f_{\boldsymbol{k}}\big)\,dt + \sigma_{\boldsymbol{k}}\,dW_{\boldsymbol{k}}(t), \tag{11}$$

where $\Omega_0$ is skew-symmetric matrix representing rotation affects, $\Gamma_0$ is a symmetric positive-definite matrix representing dissipation, and $\Sigma_0$ is a positive definite diagonal diffusion matrix. Each Fourier mode is an Ornstein-Uhlenbeck process with damping $d_{\boldsymbol{k}}$, dispersion $\omega_{\boldsymbol{k}}$, and diffusion $\sigma_{\boldsymbol{k}}$. The forcing terms $\boldsymbol{f}_0$ and $f_{\boldsymbol{k}}$ are assumed constant. The noise $W_{\boldsymbol{k}}$ is a circularly symmetric complex standard Weiner process and $\boldsymbol{W}_0$ is a real valued standard Weiner process.

The background mean $\boldsymbol{w}$ is a spatially uniform sweeping flow, which is a superposition of a constant mean sweep and a randomly fluctuating sweep, modeling large-scale motions across structures represented by $\boldsymbol{u}$, that models coherent shears and jets. The complex valued Fourier coefficients $a_{\boldsymbol{k}}$, represent time varying random velocity gradients. The proposed velocity model is exactly solvable, through standard techniques, with explicit statistics. The solution of the background mean is provided in appendix A.1 and the Fourier coefficients in appendix A.2.

The tracer particle paths are advected by the velocity field, plus a diffusion term,

$$d\boldsymbol{X}(t) = \boldsymbol{v}(\boldsymbol{X}(t),t) + \Sigma_X\,d\boldsymbol{W}_X(t), \tag{12}$$

$$= \left(\boldsymbol{w}(t) + \sum_{\boldsymbol{k}\in I_N} a_{\boldsymbol{k}}(t)\frac{i\boldsymbol{k}^{\perp}}{k} e^{i\boldsymbol{k}\cdot\boldsymbol{X}(t)}\right)dt + \Sigma_X\,d\boldsymbol{W}_X(t), \tag{13}$$

where $\boldsymbol{W}_X$ is a real valued standard Weiner process and $\Sigma_X$ is a diagonal noise matrix with $(\sigma_x, \sigma_y)$ diagonal entries. The noise can be interpreted as molecular diffusion or as an instrumental 'observation' error in the context of filtering, and we interchangeably refer to this term through either interpretation.

## 4 The aligned random turbulent shear test model for Lagrangian particles

An important special of the general velocity field in eq. (9), which we focus exclusively on, occurs when the Fourier modes are all aligned in the same direction, say $\mathbf{e}_1$, where $\mathbf{e}_i$ is a Cartesian unit vector,

$$\boldsymbol{v}(\boldsymbol{x},t) = \boldsymbol{w}(t) + u(y,t)\mathbf{e}_1. \tag{14}$$

For a shear aligned along the horizontal direction the Eulerian velocity field of the shear in eq. (9) with $\hat{\boldsymbol{k}} = \mathbf{e}_2$ satisfies

$$u(y,t) = \sum_{1\le|k|\le\Lambda} a_k(t)\frac{-ik}{|k|} e^{iky}, \quad a_k = a^*_{-k}. \tag{15}$$

The Lagrangian trajectories $\boldsymbol{X} = (X, Y)$ driven by such a flow are the solution of

$$dX(t) = \left( w_x(t) + \sum_{1 \le |k| \le \Lambda} a_k(t) \frac{-ik}{|k|} e^{ikY(t)} \right) dt + \sigma_x \, dW_x(t) \tag{16}$$

$$dY(t) = w_y(t) \, dt + \sigma_y \, dW_y(t), \tag{17}$$

where $\boldsymbol{w} = (w_x, w_y)$.

The structure of this special velocity model involves a shear along the horizontal direction, with large scale sweeping motions from $\boldsymbol{w}$. *We now study the Lagrangian and Eulerian statistics for this type of flow and explore how the sweeping and shearing components of the flow interact in determining tracer transport.*

We will show that the Lagrangian correlation function due to the shear leads to additional phase shifts from the mean $\boldsymbol{w}$ and shorter correlations due to both fluctuations of the mean $\boldsymbol{w}$ and diffusion of the vertical tracer path $\sigma_y$, when compared to the Eulerian correlation function.

## 5 Explicit Eulerian velocity and correlation function

As mentioned, the exact solution of the general velocity field, which applies to aligned shear model in section 4, is provided in appendix A. The Eulerian correlation function is the sum of the correlation function of the background mean, derived in eq. (86), and the correlation function for $u(y, t)$. Using the exact solution of each Fourier mode in appendix A.2, it is possible to show by a similar technique used to derive the temporal correlation function of each Fourier mode, that the **Eulerian correlation function** for the shear $u(y, t)$ in the equilibrium regime is homogeneous in space and stationary in time and is given by:

$$R_u(y, \tau) = \sum_{1 \le |k| \le \Lambda} \frac{\sigma_k^2}{2 d_k} e^{(-d_k - i\omega_k)\tau} e^{-iky}. \tag{18}$$

## 6 Structure and derivation of the Lagrangian velocity and correlation function

Here we first discuss the structure of the Lagrangian velocity for the shear model. We show that the special structure of the aligned shear model permits explicit formulae for the mean Lagrangian velocity and velocity fluctuations, which depend on the statistics vertical tracer paths. We use these results to derive the Lagrangian correlation function in section 6.5.

### *6.1 General structure of the Lagrangian velocity*

Recall the definition of the Lagrangian velocity field in terms of the Eulerian velocity,

$$\boldsymbol{v}^{\mathsf{L}}(\boldsymbol{\alpha}, t) = \boldsymbol{v}(\boldsymbol{X}(\boldsymbol{\alpha}, t), t) = \boldsymbol{w}(t) + u(Y(\boldsymbol{\alpha}, t), t)\mathbf{e}_1. \tag{19}$$

For the special aligned shear flow, only the vertical component of the Lagrangian tracer trajectory enters the horizontal component of the velocity field, since the vertical component is unaffected by the shear. The Eulerian and Lagrangian velocities thus coincide in the vertical direction and we can directly integrate the equations to determine the vertical particle trajectory

$$Y(\boldsymbol{\alpha}, t) = \alpha_y + \int_0^t w_y(s) \, ds + \sigma_y W_y(t), \tag{20}$$

and substitute the solution into the Eulerian shear velocity. We thus obtain that the *Lagrangian velocity* is explicitly

$$v_x^{\mathsf{L}}(\boldsymbol{\alpha}, t) = w_x(t) + \sum_{1 \le |k| \le \Lambda} a_k(t) \frac{-ik}{|k|} e^{ikY(\boldsymbol{\alpha}, t)} \tag{21}$$

$$v_y^{\mathsf{L}}(\boldsymbol{\alpha}, t) = w_y(t). \tag{22}$$

We first study the statistics of the mean vertical path, since the shear statistics depend on them. Afterwards, we utilize these results to derive the Lagrangian mean velocity. From the Lagrangian mean velocity we can then compute the Lagrangian velocity fluctuations and thus the Lagrangian correlation function, which is then explicitly computed.

### 6.2 Statistics of vertical tracer trajectories

Consider the vertical tracer trajectory. The mean of the vertical tracer path can be easily computed from

$$\overline{Y}(\boldsymbol{\alpha}, t) = \langle Y \rangle = \alpha_y + \int_0^t \langle w_y(s) \rangle \, ds, \tag{23}$$

where $\langle w_y(s) \rangle$ is given in eq. (83). Assuming the velocity field is in the statistically stationary regime, where $\overline{w} = -f_0/p_0$, we then find that the vertical tracer mean is

$$\overline{Y}(\boldsymbol{\alpha}, t) = \alpha_y + \overline{w}_y t, \quad \text{where } \overline{w}_y = \mathrm{Im}\{-f_0/p_0\} = \frac{d_0 f_{0y} + \omega_0 f_{0x}}{d_0^2 + \omega_0^2}, \tag{24}$$

which grows linearly in time $\overline{Y} \sim t$. To compute the variance $\sigma_Y^2(t)$, we first compute the equations for the deviations from its mean

$$\widetilde{Y}(\boldsymbol{\alpha}, t) = Y - \langle Y \rangle = \int_0^t \widetilde{w}_y(s) \, ds + \sigma_y \int_0^t dW_y(s), \tag{25}$$

where $\widetilde{w}_y(t) = \mathrm{Im}\{w(t) - \langle w(t) \rangle\}$. Next,

$$\sigma_Y^2(t) = \langle \widetilde{Y}^2 \rangle = \sigma_w^2(t) + \sigma_y^2 t = 2 \int_0^t (t - \tau) R_{w_y}(\tau) \, d\tau + \sigma_y^2 t, \tag{26}$$

and since the diffusion matrix $\Sigma_0$ has diagonal entries that are equivalent and equal to $\sigma_0$ and the noise is circularly symmetric, the correlation of $w_y(t)$ is equal to half the real part of the correlation of the complex process $w(t)$ in eq. (86). Explicit integration shows,

$$\begin{aligned} \sigma_w^2(t) &= 2 \int_0^t (t - \tau) R_{w_y}(\tau) \, d\tau \\ &= \frac{\sigma_0^2}{d_0 (d_0^2 + \omega_0^2)^2} \Big( (-d_0^2 + \omega_0^2) + e^{-d_0 t} \big( (d_0^2 - \omega_0^2) \cos(\omega_0 t) - 2 d_0 \omega_0 \sin(\omega_0 t) \big) \Big) + \left( \frac{\sigma_0^2}{(d_0^2 + \omega_0^2)} \right) t. \end{aligned} \tag{27}$$

For the case with zero rotation in the background mean $\omega_0 = 0$, the tracer dispersion simplifies to

$$\sigma_Y^2(t) = \Big( \frac{\sigma_0^2}{d_0^2} + \sigma_y^2 \Big) t + \frac{\sigma_0^2}{d_0^3} (e^{-d_0 t} - 1). \tag{28}$$

The long and short time behavior for the case with non-zero rotation is given by

$$\sigma_Y^2 \sim \sigma_y^2 t + \frac{\sigma_0^2}{2 d_0} t^2 \quad \text{for small } t, \qquad \sigma_Y^2 \sim \left( \frac{\sigma_0^2}{(d_0^2 + \omega_0^2)} + \sigma_y^2 \right) t \quad \text{for large } t. \tag{29}$$

At long times we have linear or diffusive growth of the tracer variance. We find that rotation reduces the diffusion rate at long times $t \gg d_0$, but does not manifest at short times. We also note when the diffusion term is zero $\sigma_y = 0$, the tracer grows at a ballistic rate at short times $t \ll d_0$, but when the molecular diffusion is non-zero, the variance grows linearly.

### 6.3 Equations for the mean Lagrangian velocity

Consider now the mean Lagrangian velocity. Taking the ensemble mean of the Lagrangian velocity leads to the mean velocities:

$$\overline{v}_x^{\mathsf{L}}(\boldsymbol{\alpha}, t) = \overline{w}_x + \sum_{1 \le |k| \le \Lambda} \frac{-ik}{|k|} \Big\langle a_k(t) e^{ikY(\boldsymbol{\alpha}, t)} \Big\rangle, \tag{30}$$

$$\overline{v}_y^{\mathsf{L}}(\boldsymbol{\alpha}, t) = \overline{w}_y. \tag{31}$$

We now simplify the ensemble average that appears above. Recall that the characteristic function of a random variable $Y$ is defined as $\phi_Y(t) = \langle e^{itY} \rangle$. Explicit computation for a Gaussian random variable shows

$$\phi_Y(t) = e^{i \langle Y \rangle t - \frac{1}{2} \mathrm{Var}(Y) t^2}. \tag{32}$$

Since the drifter trajectory in the vertical direction $Y$ is Gaussian, and since $a_k$ is independent of $Y$,

$$\left\langle a_k(t)e^{ikY(\boldsymbol{\alpha},t)}\right\rangle = \langle a_k(t)\rangle e^{ik\langle Y(\boldsymbol{\alpha},t)\rangle - \frac{1}{2}k^2\,\mathrm{Var}(Y(\boldsymbol{\alpha},t))} = \overline{a_k}e^{ik\overline{Y}(\boldsymbol{\alpha},t)-\frac{1}{2}k^2\sigma_Y^2(t)}. \tag{33}$$

where $\sigma_Y^2(t) = \mathrm{Var}(Y(\boldsymbol{\alpha},t))$. Substituting the equations for the mean of the shear mode and the vertical particle mean and variance from section 6.2, we find that the mean Lagrangian velocity is explicitly

$$\overline{v}_x^{\mathsf{L}}(\boldsymbol{\alpha},t) = \overline{w}_x + \sum_{1\le|k|\le\Lambda}\frac{ik}{|k|}\frac{f_k}{p_k}e^{ik(\alpha_y+\overline{w}_y t)-\frac{1}{2}k^2\sigma_Y^2(t)}, \tag{34}$$

$$\overline{v}_y^{\mathsf{L}}(\boldsymbol{\alpha},t) = \overline{w}_y. \tag{35}$$

### *6.4 Equations for the Lagrangian velocity fluctuations*

Computing $\widetilde{\boldsymbol{v}}^{\mathsf{L}} = \boldsymbol{v}^{\mathsf{L}} - \overline{\boldsymbol{v}}^{\mathsf{L}}$, using the results from the Lagrangian mean calculations, we find that the Lagrangian velocity fluctuations are governed by

$$\widetilde{v}_x^{\mathsf{L}}(\boldsymbol{\alpha},t) = \widetilde{w}_x(t) + \sum_{1\le|k|\le\Lambda}e^{ik\langle Y(\boldsymbol{\alpha},t)\rangle}\frac{-ik}{|k|}\Big(a_k(t)e^{ik\widetilde{Y}(\boldsymbol{\alpha},t)} - \overline{a_k}e^{-\frac{1}{2}k^2\,\mathrm{Var}(Y(\boldsymbol{\alpha},t))}\Big), \tag{36}$$

$$\widetilde{v}_y^{\mathsf{L}}(\boldsymbol{\alpha},t) = \widetilde{w}_y(t). \tag{37}$$

### *6.5 Explicit Lagrangian correlation function along the shearing direction*

Next we consider the Lagrangian correlation function $R^{\mathsf{L}^2}$. To proceed, note we have already derived the correlation function of the background velocity $\boldsymbol{w}$ and what remains is to determine the Lagrangian correlation of the shear term $u(y,t)$.

Consider the structure of the Lagrangian velocity

$$\boldsymbol{v}^{\mathsf{L}}(\boldsymbol{\alpha},t) = \boldsymbol{w}(t) + u(Y(\boldsymbol{\alpha},t),t)\mathbf{e}_1, \tag{38}$$

the correlation of the Lagrangian velocity has the form

$$R^{\mathsf{L}^2}(\boldsymbol{\alpha}_1,\boldsymbol{\alpha}_2,t,t') = R_{\boldsymbol{w}}(t,t') + R_u^{\mathsf{L}^2}(\boldsymbol{\alpha}_1,\boldsymbol{\alpha}_2,t,t')\mathbf{e}_1\mathbf{e}_1^*. \tag{39}$$

The unknown term $R_u^{\mathsf{L}^2}$ is given by,

$$R_u^{\mathsf{L}^2}(\boldsymbol{\alpha}_1,\boldsymbol{\alpha}_2,t,t') = \big\langle\widetilde{u}\big(Y(\boldsymbol{\alpha}_1,t),t\big)\widetilde{u}\big(Y(\boldsymbol{\alpha}_2,t'),t'\big)^*\big\rangle \tag{40}$$

$$= \left\langle\widetilde{u}\left(\alpha_{y1}+\int_0^t w_y(s)\,ds+\sigma_y W_y(t),t\right)\times\widetilde{u}\left(\alpha_{y2}+\int_0^{t'}w_y(s)\,ds+\sigma_y W_y(t'),t'\right)^*\right\rangle. \tag{41}$$

We can simplify the above expression using the formula for the Lagrangian fluctuations in section 6.4, explicitly, or by application of the total law of expectations. We show the derivation using the total law of expectations. In particular, using the total law of expectations, we can first fix the random term $w_y$, take the expectation over the noise, and then take a second expectation over $w_y$ to obtain $R_u^{\mathsf{L}^2}$. The first expectation relates the Lagrangian correlation function to the Eulerian correlation function given in eq. (18):

$$R_u^{\mathsf{L}^2}(\boldsymbol{\alpha}_1,\boldsymbol{\alpha}_2,t,t') = \big\langle R_u(Y(\boldsymbol{\alpha}_1,t),Y(\boldsymbol{\alpha}_2,t'),t,t')\big\rangle \tag{42}$$

$$= \left\langle\sum_{1\le|k|\le\Lambda}\frac{\sigma_k^2}{2d_k}e^{-d_k(t'-t)}e^{-i\omega_k(t'-t)}e^{-ik(Y(\boldsymbol{\alpha}_2,t')-Y(\boldsymbol{\alpha}_1,t))}\right\rangle \tag{43}$$

$$= \left\langle\sum_{1\le|k|\le\Lambda}\frac{\sigma_k^2}{2d_k}e^{-d_k(t'-t)}e^{-i\omega_k(t'-t)}e^{-ik(\alpha_{y2}-\alpha_{y1})}e^{-ik\left(\int_t^{t'}w_y(s)\,ds+\int_t^{t'}\sigma_y\,dW_y\right)}\right\rangle. \tag{44}$$

Next let $t' = t+\tau$ and since the trajectory $Y(\boldsymbol{\alpha},t)$ only depends on the initial condition in the $y$ coordinate, we denote the difference between $\boldsymbol{\alpha}_2$ and $\boldsymbol{\alpha}_1$ by $y$, thus

$$R_u^{\mathsf{L}^2}(y,t,t+\tau) = \sum_{1\le|k|\le\Lambda}\frac{\sigma_k^2}{2d_k}e^{-d_k\tau}e^{-i\omega_k\tau}e^{-iky}\left\langle e^{-ik\left(\int_t^{t+\tau}w_y(s)\,ds+\int_t^{t+\tau}\sigma_y\,dW_y\right)}\right\rangle. \tag{45}$$

We can now apply the result for the characteristic function of a Gaussian random variable again and use the results for the mean and variance of the vertical tracer trajectory to simplify the ensemble mean that appears in the equation above. We obtain that the *Lagrangian correlation function* is

$$R_u^{\mathsf{L}_2}(y,\tau) = \sum_{1\le|k|\le\Lambda} \frac{\sigma_k^2}{2d_k} e^{-d_k\tau} e^{-i\omega_k\tau} e^{-iky} e^{-ik\overline{w}_y\tau} e^{-\frac{1}{2}k^2\sigma_Y^2(\tau)}, \tag{46}$$

where $\sigma_Y^2$ and $\overline{w}_y$ are given explicitly in section 6.2. The Lagrangian autocorrelation function is obtained by setting $y = 0$.

$$R_u^{\mathsf{L}}(\tau) = \sum_{1\le|k|\le\Lambda} \frac{\sigma_k^2}{2d_k} e^{-d_k\tau} e^{-i\omega_k\tau} e^{-ik\overline{w}_y\tau} e^{-\frac{1}{2}k^2\sigma_Y^2(\tau)}. \tag{47}$$

## 7 Comparison of the Lagrangian and Eulerian statistics along the shearing direction

Before studying the dispersive properties of Lagrangian particles along the shear, we highlight and discuss the differences between the Eulerian and Lagrangian correlation functions.

Consider a model with a single shear mode. Recall that the Eulerian correlation, from eq. (18), at a fixed location in space is given by

$$R_u(\tau) = \frac{\sigma_k^2}{d_k} e^{-d_k\tau}\cos(\omega_k\tau), \tag{48}$$

and the Lagrangian correlation following a single particle in space, from eq. (46) with $y = 0$, assuming a deterministic mean so that $\sigma_Y^2(t) = \sigma_y^2 t$, is

$$R_u^{\mathsf{L}}(\tau) = \frac{\sigma_k^2}{d_k} e^{-(d_k+\frac{1}{2}k^2\sigma_y^2)\tau}\cos((\omega_k + k\overline{\omega}_y)\tau). \tag{49}$$

The difference between the Eulerian and Lagrangian correlation functions for a non-dispersive mode with $\omega_k = 0$ is given by

$$|R_u - R_u^{\mathsf{L}}| = R_u \times \left(1 - e^{-\frac{1}{2}k^2\sigma_y^2\tau}\cos(k\overline{\omega}_y\tau)\right). \tag{50}$$

A comparison is shown in fig. 1. Observe how the sweeping motion of the background mean affects the Lagrangian velocity statistics with faster decaying correlations that oscillate more rapidly, compared to the Eulerian statistics. The strength of the vertical mean impacts the strength of the oscillations and the properties of the molecular diffusion affect how rapidly the correlations decay. Flows with a strong vertical mean have rapidly oscillating Lagrangian correlations. And flows with a strongly energetic mean and large molecular diffusion have short correlations with rapid decay. Furthermore, for flows with a mean, the correlations are closest at every $2\pi/k\overline{w}_y$ periods in a single mode system. These factors result in large differences between the Eulerian and Lagrangian correlation functions, and in summary

- Flows with a strong vertical mean results in correlations with rapid oscillations.
- Flows with a strong energetic mean and large particle molecular diffusion have short range correlations that rapidly decay.

In the next section, we discuss the physical interpretation that cause the difference between the Lagrangian and Eulerian statistics, which stem from an interplay between the mean sweeps and the shear flow.

## 8 Lagrangian statistics and mixing behavior along the shearing direction

We derive equations that predict the mixing behavior or tracer dispersion along the shearing direction in various limits. We later link these predictions with numerical simulations where various terms dominate in section 9, referring back to the discussion here.

We first discuss models with a purely deterministic mean, where an explicit formula can be derived for the tracer dispersion. This is developed for a single shear mode in section 8.1 and the general case in section 8.2; we then discuss and interpret the results in section 8.2.1. For a general random background mean, we derive the dispersion characteristics in the short and long time limits in section 8.3, where we also discuss the new physics that arises in this more general case.

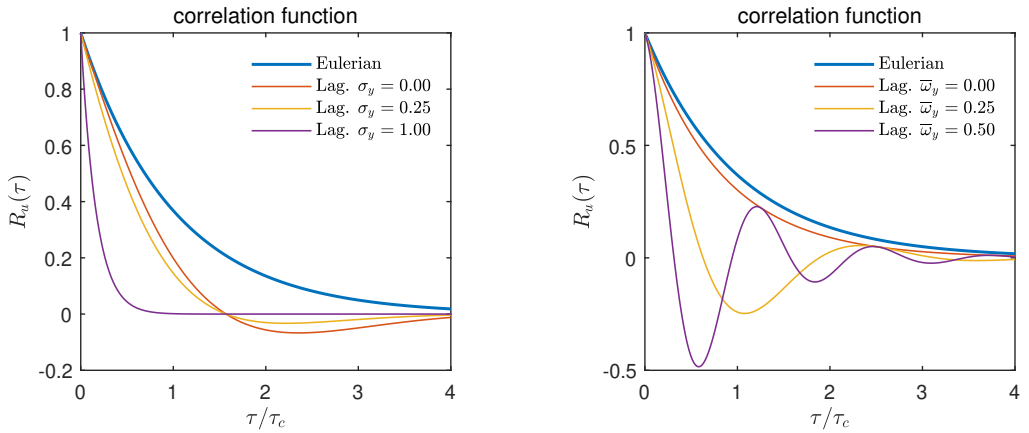


**(a)** Fixed $\overline{w}_y = 0.1$ and varying $\sigma_y$.

**(b)** Fixed $\sigma_y = 0.2$ and varying $\overline{w}_y$.

**Figure 1** Comparison of the Eulerian (solid blue) and Lagrangian correlation function as the model mean and molecular diffusion are varied. Here $\tau_c = 1/\nu$, where $\nu$ is the model viscosity (see section 9).

### *8.1 A single shear mode with a constant background mean*

The simplest setting involves a single shear mode and a deterministic sweep. In this setting the vertical tracer variance is simply $\sigma_Y^2(t) = \sigma_y^2 t$ and the reduced equation for the autocorrelation function for the tracer along the shearing direction simplifies to

$$R_u^{\mathsf{L}}(\tau) = \frac{\sigma_k^2}{2d_k} 2\,\mathrm{Re}\{e^{-d_k\tau} e^{-i\omega_k\tau} e^{-ik\overline{w}_y\tau} e^{-\frac{1}{2}k^2\sigma_y^2\tau}\}. \tag{51}$$

We define an *effective damping and dispersion* by

$$\tilde{d}_k = d_k + \frac{1}{2}k^2\sigma_y^2 \quad \text{and} \quad \tilde{\omega}_k = \omega_k + k\overline{w}_y, \tag{52}$$

respectively, then

$$R_u^{\mathsf{L}}(\tau) = \frac{\sigma_k^2}{d_k}\,\mathrm{Re}\{e^{(-\tilde{d}_k - i\tilde{\omega}_k)\tau}\}. \tag{53}$$

The Lagrangian particle variance from the shear term is obtained by integration

$$\begin{aligned}\sigma_u^2(t) &= 2\int_0^t (t-\tau) R_u^{\mathsf{L}}(\tau)\, d\tau \\ &= \frac{2\sigma_k^2}{(\tilde{d}_k^2 + \tilde{\omega}_k^2)} t + \frac{2\sigma_k^2}{d_k(\tilde{d}_k^2 + \tilde{\omega}_k^2)^2}\left((-\tilde{d}_k^2 + \tilde{\omega}_k^2) + e^{-\tilde{d}_k t}((\tilde{d}_k^2 - \tilde{\omega}_k^2)\cos(\tilde{\omega}_k t) - 2\tilde{d}_k\tilde{\omega}_k \sin(\tilde{\omega}_k t))\right).\end{aligned} \tag{54}$$

The last contribution to the variance involves the diffusion term from the Brownian noise term,

$$\sigma_X^2(t) = \sigma_u^2(t) + \sigma_x^2 t, \tag{55}$$

and thus the behavior of the tracer dispersion along the shear in total is governed by

$$\sigma_u^2 \sim \sigma_x^2 t + \frac{\sigma_k^2}{d_k} t^2 \quad \text{for small } t \quad \text{and} \quad \sigma_u^2 \sim \left(\frac{2\sigma_k^2}{\tilde{d}_k^2 + \tilde{\omega}_k^2} + \sigma_x^2\right) t \quad \text{for large } t. \tag{56}$$

### *8.2 General shear flows with a constant background mean*

For multiple shear modes, the result is identical to the single shear mode case except the contribution due to all the various modes is summed. The total variance from the shearing flow is therefore

$$\sigma_u^2(t) = \sum_{1\le k\le\Lambda} \frac{2\sigma_k^2}{d_k(\tilde{d}_k^2 + \tilde{\omega}_k^2)^2}\left((-\tilde{d}_k^2 + \tilde{\omega}_k^2) + d_k(\tilde{d}_k^2 + \tilde{\omega}_k^2)t + e^{-\tilde{d}_k t}((\tilde{d}_k^2 - \tilde{\omega}_k^2)\cos(\tilde{\omega}_k t) - 2\tilde{d}_k\tilde{\omega}_k \sin(\tilde{\omega}_k t))\right). \tag{57}$$

Where the total variance of $X$ trajectories is again given by $\sigma_X^2(t) = \sigma_u^2(t) + \sigma_x^2 t$. The tracer variance has the following short and long time behavior

$$\sigma_X^2 \sim \sigma_x^2 t + \sum_{1\le k\le \Lambda} \frac{\sigma_k^2}{d_k} t^2 \quad \text{for small } t, \quad \sigma_X^2 \sim \left( \sum_{1\le k\le \Lambda} \frac{2\sigma_k^2}{\tilde{d}_k^2 + \tilde{\omega}_k^2} + \sigma_x^2 \right) t \quad \text{for large } t. \tag{58}$$

*8.2.1 Mixing behavior in various limits*

We make the following observations regarding the tracer variance behavior.

- At small times, if the tracer particles are driven by molecular diffusion $\sigma_x$, diffusion dominates over the ballistic growth rate due to the shear. When there is zero molecular diffusion $\sigma_x = 0$, the tracer variance grows at a ballistic rate.
- Assume zero molecular diffusion and a shear with a power law spectrum $E_k = \mathcal{E}|k|^{-\alpha}$, we then find the short time behavior is given by

  $$\sigma_X^2 \sim \left( 2\mathcal{E} \sum_{1\le k\le \Lambda} |k|^{-\alpha} \right) t^2, \tag{59}$$

  hence the diffusion is determined entirely by the spectral slope from the shearing component when $\sigma_x = 0$.
- At long times, the behavior of the tracer along the shearing direction is diffusive. To understand the affects of each term, consider the effective damping and dispersion

  $$\tilde{d}_k = d_k + \frac{1}{2}\sigma_y^2 k^2 \quad \text{and} \quad \tilde{\omega}_k = \omega_k + k\overline{w}_y. \tag{60}$$

  For simplicity, consider a scenario with non-dispersive modes $\omega_k = 0$ and viscous damping $d_k = \mu k^2$, we then find that the dispersion due to the shear is

  $$\sigma_X^2 \sim \left( \sum_{1\le k\le \Lambda} \frac{4\mu\mathcal{E}|k|^{-\alpha}}{(\mu + \frac{1}{2}\sigma_y^2)^2 k^2 + \overline{\omega}_y^2} + \sigma_x^2 \right) t. \tag{61}$$

  Observe that the cross sweeps lead to reduced dispersion rates, which we expect since the cross sweeps push particles across streamlines and thus impede them from dispersing along the shearing direction. We also see how molecular diffusion along the vertical direction leads to enhanced viscosity, through a similar mechanism as described for the cross sweeps, but which is scale dependent.

  For large wavenumbers the effective contribution to the dispersion is minimal since

  $$\frac{4\mu\mathcal{E}|k|^{-\alpha}}{(\mu + \frac{1}{2}\sigma_y^2)^2 k^2 + \overline{\omega}_y^2} \sim \frac{4\mu\mathcal{E}}{(\mu + \frac{1}{2}\sigma_y^2)^2} |k|^{-\alpha-2}, \quad \text{for large } k. \tag{62}$$

  Consider the scenario where the viscosity is large relative to the cross sweeps and tracer diffusion, i.e. minimal magnitude cross sweeps, we find that shear variance is given by

  $$\sigma_u^2 \sim \left( \sum_{1\le k\le \Lambda} \frac{4\mathcal{E}}{\mu} |k|^{-\alpha-2} \right) t, \quad \text{for large } \mu, \tag{63}$$

  which is the scenario where $Y$ has a minimal contribution to the Lagrangian velocity.
- An elementary observation is that the effective reduction on the dispersion rate due to cross sweeps is mitigated if the shear is dispersive. In the extreme scenario, it can be suppressed by advection with speed $c = \overline{w}_y$ and $\omega_k = -ick$. When the cross sweeps are zero, the diffusion rate is only reduced due to contributions from molecular diffusion from vertical tracer paths.

### *8.3 Shear flows with a general random background mean: short and long time behavior*

Now consider the most general case involving random cross sweeps with a mean. For now consider a single shear mode, the Lagrangian autocorrelation is then given by

$$R_u^{\mathsf{L}}(\tau) = \frac{\sigma_k^2}{2d_k} 2\,\mathrm{Re}\{e^{-d_k\tau}e^{-i\omega_k\tau}e^{-ik\overline{w}_y\tau}e^{-\frac{1}{2}k^2\sigma_Y^2(\tau)}\}, \tag{64}$$

where the variance of the vertical tracer dispersion has been computed as

$$\sigma_Y^2(t) = \sigma_w^2(t) + \sigma_y^2 t, \tag{65}$$

where $\sigma_w^2$ is given in eq. (27). Integrating, the resulting autocorrelation function is unwieldy for the full $\sigma_u^2$, we instead study the behavior of the tracer variance at short and long times. To proceed, recall the behavior of the vertical tracer variance in these limits from eq. (29),

$$\sigma_Y^2 \sim \sigma_y^2 t + \frac{\sigma_0^2}{2d_0}t^2 \quad \text{for small } t, \qquad \sigma_Y^2 \sim \left(\frac{\sigma_0^2}{(d_0^2+\omega_0^2)} + \sigma_y^2\right)t \quad \text{for large } t. \tag{66}$$

#### *8.3.1 Short time behavior*

At short times the diffusion rate, for zero molecular diffusion, is again dominated by Brownian noise at a linear rate determined by $\sigma_x$. The effective damping and dispersion in the short time limit is given by

$$\tilde{d}_k = d_k + \frac{1}{2}\sigma_y^2 k^2 \quad \text{and} \quad \tilde{\omega}_k = \omega_k + \overline{w}_y k. \tag{67}$$

At these time scales the effects of the random cross sweeps do not manifest. The autocorrelation function of a single shear mode is thus

$$R_u^{\mathsf{L}}(\tau) = \frac{\sigma_k^2}{d_k}\,\mathrm{Re}\{e^{(-\tilde{d}_k - i\tilde{\omega}_k)\tau}e^{-\frac{1}{2}\frac{\sigma_0^2}{2d_0}\tau^2}\}, \tag{68}$$

and an expansion at small times shows that the dispersion due to the shear is identical to the deterministic cross sweep scenario; hence, the variance at short times has the scaling

$$\sigma_X^2 \sim \sigma_x^2 t + \left(\frac{\sigma_0^2}{(d_0^2+\omega_0^2)} + 2\mathcal{E}\sum_{1\le k\le\Lambda}|k|^{-\alpha}\right)t^2 \quad \text{for small } t. \tag{69}$$

#### *8.3.2 Long time behavior*

In the large time limit, we find that the effective damping and dispersion are

$$\tilde{d}_k = d_k + \frac{1}{2}\sigma_y^2 k^2 + \frac{\sigma_0^2}{2(d_0^2+\omega_0^2)}k^2 \quad \text{and} \quad \tilde{\omega}_k = \omega_k + \overline{w}_y k. \tag{70}$$

The additional term above, due the random mean, in the effective damping acts identical to viscous damping. For the total tracer variance, we must also include the additional contribution due to the sweeping term to the shearing variance of the particle, which is $\sigma_w^2$ and is equivalent to the vertical component given in eq. (27):

$$\sigma_X^2(t) = \sigma_w^2(t) + \sigma_u^2(t) + \sigma_x^2 t. \tag{71}$$

For the shear term above, the result from section 8.2, but with the appropriate effective damping and dispersion defined eq. (70). We thus find that the total variance scales like

$$\sigma_X^2 \sim \left(\frac{\sigma_0^2}{(d_0^2+\omega_0^2)} + \sum_{1\le k\le\Lambda}\frac{2\sigma_k^2}{\tilde{d}_k^2+\tilde{\omega}_k^2} + \sigma_x^2\right)t \quad \text{for large } t. \tag{72}$$

The same observations and intuition holds here as for the case with deterministic cross sweeps at long times (see section 8.2.1), but with enhanced damping due to the random component of the mean.

If we again consider a model with viscous damping $d_k = \mu k^2$ and zero dispersion we find that variance due to the shear at long times scales like

$$\sigma_u^2 \sim \Big( \sum_{1 \le k \le \Lambda} \frac{4\mu \mathcal{E} |k|^{-\alpha}}{(\mu + \frac{1}{2}\sigma_y^2 + \frac{\sigma_0^2}{2(d_0^2+\omega_0^2)})^2 k^2 + \overline{\omega}_y^2} \Big) t. \tag{73}$$

Observe that the affects of the random component of the mean enter the shear dispersion rate at long times. We make the following important observation regarding the background mean and its interaction with the shear:

- Random background fluctuations reduce dispersive mixing along the shear. A highly energetic background impedes particles from dispersion along the shear; the random fluctuations constrain the particles from free advection by the shear.
- Large rotation $\omega_0$ enhances dispersion along the shear. Physically, strong rotation forces particles to rotate counterclockwise pushing them across streamlines as they are randomly swept along by the shear, which counteracts the noise in the mean preventing the particles from dispersing; the combined affect of this interplay leads to enhanced dispersion.
- A random mean with a small time correlations, i.e. large damping $d_0 \gg 0$, acts on particles on very short time scales, which minimizes the impact of the random mean term, thus enhancing the mixing rate. Conversely a mean with long time correlations, i.e. small damping $d_0 \ll 0$, blocks the shear and reduces the dispersion rate.

## 9 Numerical simulation of model regimes and tracer dispersion statistics

Here we include numerical simulation in different model regimes and compare tracer dispersion statistics with theoretical predictions. We study important physical features that arise when certain model parameters dominate, and connect them with the discussion in section 8.

Consider the aligned shear model described in section 4,

$$\boldsymbol{v}(\boldsymbol{x}, t) = \boldsymbol{w}(t) + u(y, t)\mathbf{e}_1, \tag{74}$$

where the spatial mean is given by,

$$dw = \big((-d_0 + i\omega_0)w + f_0\big)dt + \sqrt{2}\sigma_0 \, dW_0, \tag{75}$$

and where the shear satisfies

$$u(y,t) = \sum_{1 \le |k| \le \Lambda} a_k(t) \frac{-ik}{|k|} e^{iky}, \quad a_k = a_{-k}^*, \tag{76}$$

$$da_k = \big((-d_k + i\omega_k)a_k + f_k\big)\, dt + \sigma_k \, dW_k. \tag{77}$$

The time scale of the flow is defined by $\tau_c = 1/\mu$ and the damping model is given by $d_k = \mu k^2$. The simulation length is $t = 600\,\tau_c$ and $L = 250$ drifter ensembles are used. We assume particle diffusion is equivalent in both directions, i.e. $\sigma_X = \sigma_x = \sigma_y$. The forcing is specified as $f_0 = f_{0x} + if_{0y}$, with $f_{0x} = 0$. We consider a model with maximum wavenumber $\Lambda = 10$ and a spectrum with $E_k = \mathcal{E}|k|^{-\alpha}$, where $\mathcal{E} = 1.0$. Examples are included where we vary the energy of the fluctuations of the background mean defined by $E_0 = \sigma_0^2/2d_0$.

### *9.1 Numerical simulations in various test regimes*

In the following figures, 10 tracer trajectories are plotted over a simulation length of $40\,\tau_c$ units. The simulation domain is a $2\pi$ periodic box, however we 'unwrap' the tracers trajectories over the periodic domain to demonstrate their spatial extent. In the tracer variance figures, the dashed red line corresponds to the prediction in eq. (69) and the solid red line to the prediction eq. (72). Note the close agreement with the predicted diffusion rates and those obtained by Monte-Carlo simulations in all regimes.

#### *9.1.1 Particle diffusion magnitude*

We compare cases in figs. 2 and 3 for varying tracer diffusion value in regimes with a small constant mean sweep. Observe how larger values of the diffusion $\sigma_X$ (recall $\sigma_y = \sigma_X$) constrain the tracer trajectories from freely mixing

and slow down overall mixing, see also eq. (61). The long term mixing rate rate for the example with smaller molecular diffusion $\sigma_X = 0.05$ is $D = 47$, whereas the example with large diffusion $\sigma_X = 0.8$ the long term mixing rate $D = 5.4$.

**Figure 2** $\sigma_X = 0.05$

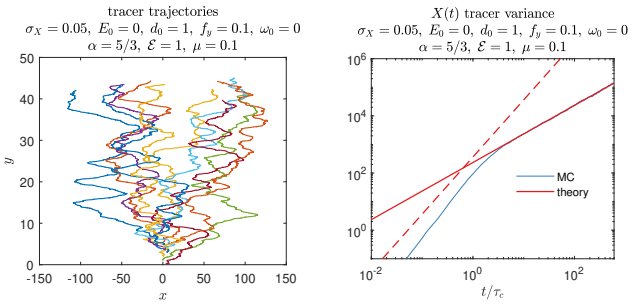


**Figure 3** $\sigma_X = 0.8$

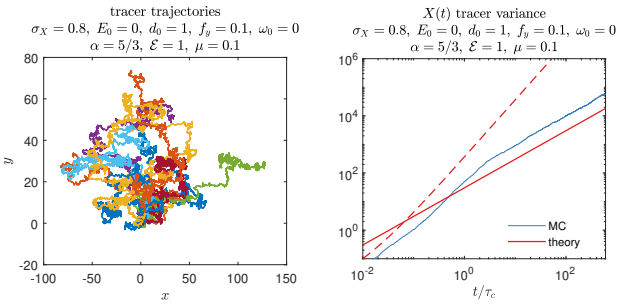


### *9.1.2 Model forcing*

We demonstrate an example in fig. 4 with a non-uniform spatially mean by forcing the three most energetic shear modes, for a regime with a small constant mean sweep and small particle diffusion magnitude. The model forcing generates a coherent jet-like flow. Forcing does not impact the dispersion rate compared to unforced models. The main observation is the large pre-constant at short times, which is due to the jet and the uniform distribution of the particles at $t = 0$.

**Figure 4** $f_1 = 1.0,\ f_2 = 2.0,\ f_3 = 2.0$

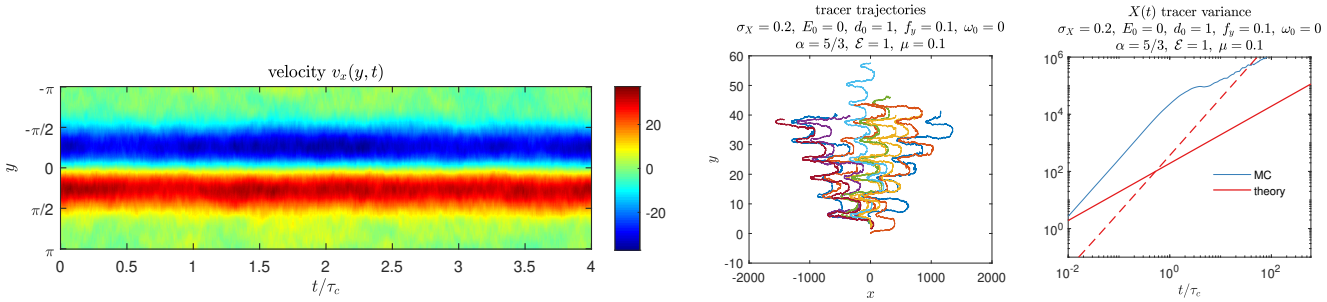


### *9.1.3 Spectral slope*

In the examples in figs. 5 and 6, we compare varying the spectral slope (shear energy) of the model for regimes with a small constant mean sweep, small particle diffusion magnitude, and no background mean rotation term. A more energetic spectrum leads to more violent velocity fields and the tracer trajectories are thus more energetic with greater mixing rates compared to cases with steeper spectra, where the energy of the smallest scales are comparatively weaker. However, the differences between these two examples are not as pronounced since the dependence on the mixing rate for large wavenumbers is reduced at long times, see eq. (62). The short time behavior is more greatly impacted by the spectral slope, see eq. (59), especially for small magnitudes of particle molecular diffusion.

**Figure 5** $E_k \propto |k|^{-3}$

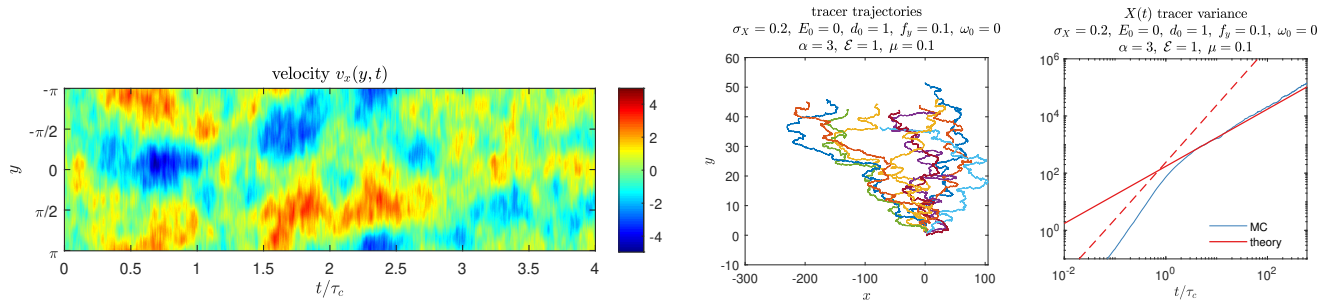

**Figure 6** $E_k \propto |k|^{-1}$

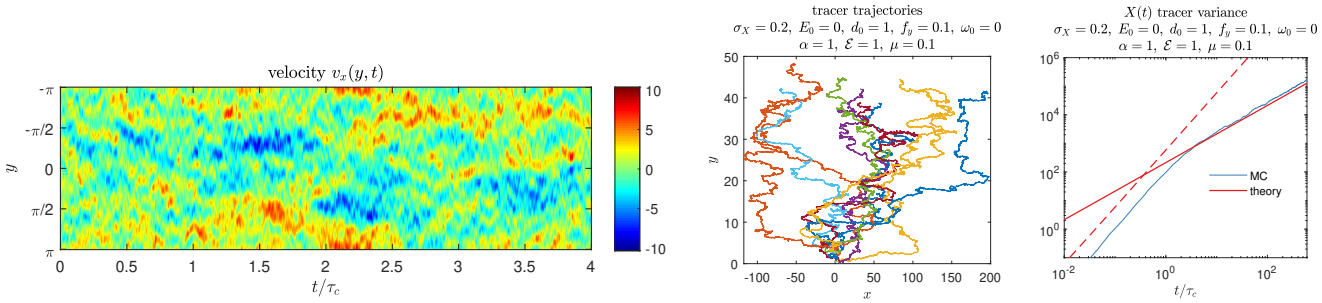


### *9.1.4 Constant background mean magnitude*

For the examples in figs. 7 and 8, the constant mean sweep strength is varied for regimes with small particle diffusion magnitudes. We see how a strong mean impedes dispersion, since the affects of the shear on tracer particles is greatly reduced. In particular, note the scale of the vertical and horizontal axes. The strong vertical mean with $\overline{w}_y = 2$ results in particles looping around periodic box 20 times more than when $\overline{w}_y = 0.1$. In addition, particles under the strong mean case are trapped and have restricted horizontal extent, which results in reduced dispersion rates along the shear.

**Figure 7** $\overline{w}_y = 0.1$

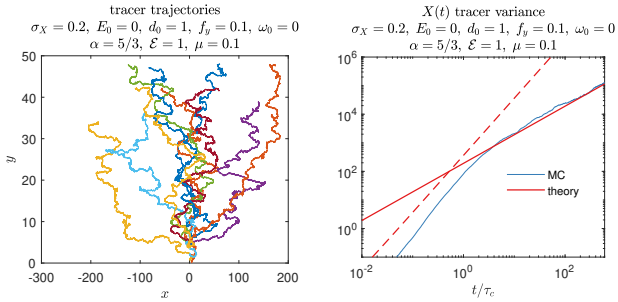


**Figure 8** $\overline{w}_y = 2$

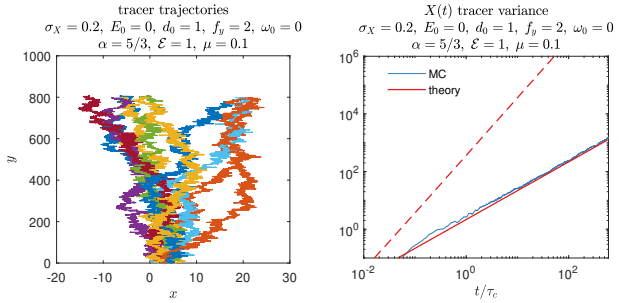


### *9.1.5 Random background mean*

We discuss examples now with a random background mean, which introduces new physical features. Compare figs. 9 and 10, where we see that a highly energetic mean results in prominent vertical striations in the Eulerian velocity field. As discussed in section 8.3, an energetic background impedes tracers from advection along the shear and reduces the overall mixing rate, as observed in the test regimes.

In figs. 9 and 11, we fix the background energy level $E_0$, and show the affects of varying the time scale of the background fluctuations by changing the damping $d_0$. Observe how large damping values (short time correlations) results in increased mixing rates, since then the mean fluctuations act on very short time scales and effectively diminish the affects of the random fluctuations on reducing dispersion rates. Conversely, observe how small damping (long time correlations) act to suppress mixing.

Fig. 12 demonstrates an example with strong rotation $\omega_0$. Observe that an oscillating background mean result in greater mixing compared to the conditions without a mean in fig. 9, even though in both cases the mean has equivalent energy. As mentioned in section 8.3 a rotating mean results in particles meandering along the shear and counteracts the noise in the mean, which tries to prevent the particles from dispersing.

**Figure 9** $E_0 = 0.1,\ d_0 = 1,\ \omega_0 = 0$

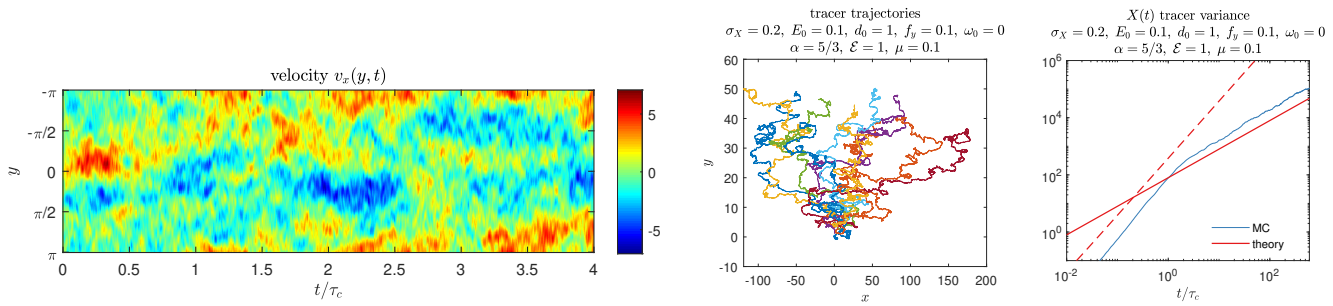


**Figure 10** $E_0 = 1,\ d_0 = 1,\ \omega_0 = 0$

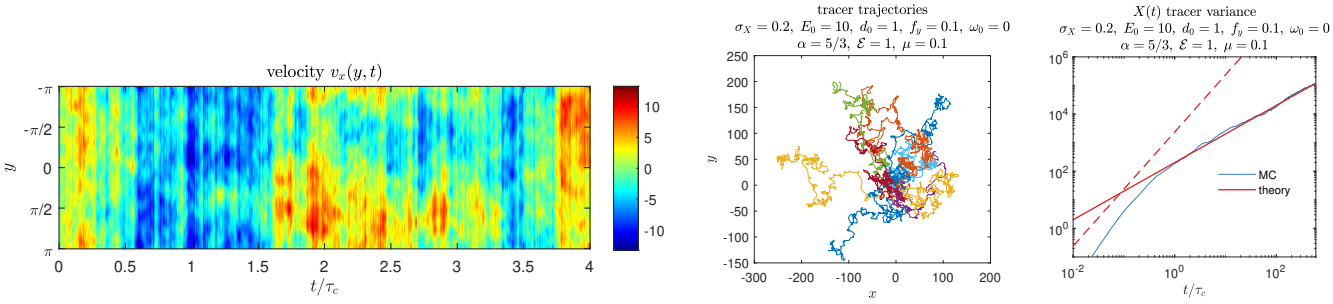


**Figure 11** $E_0 = 0.1, d_0 = 10,\ \omega_0 = 0$

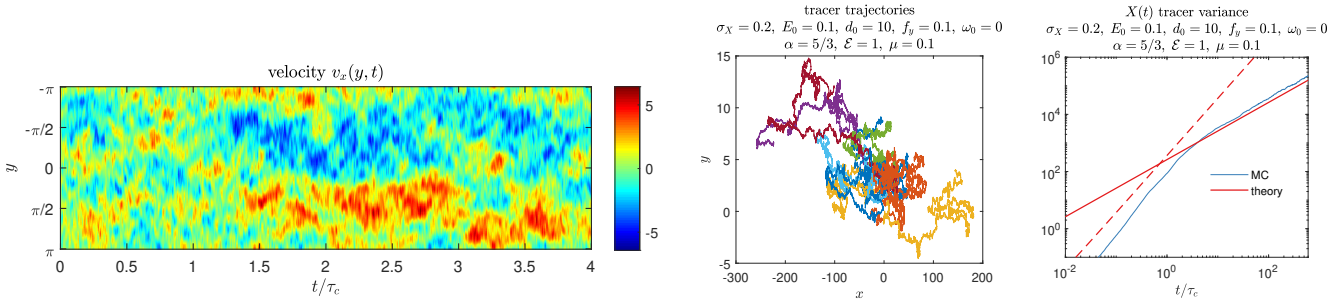


**Figure 12** $E_0 = 0.1, d_0 = 1,\ \omega_0 = 10$

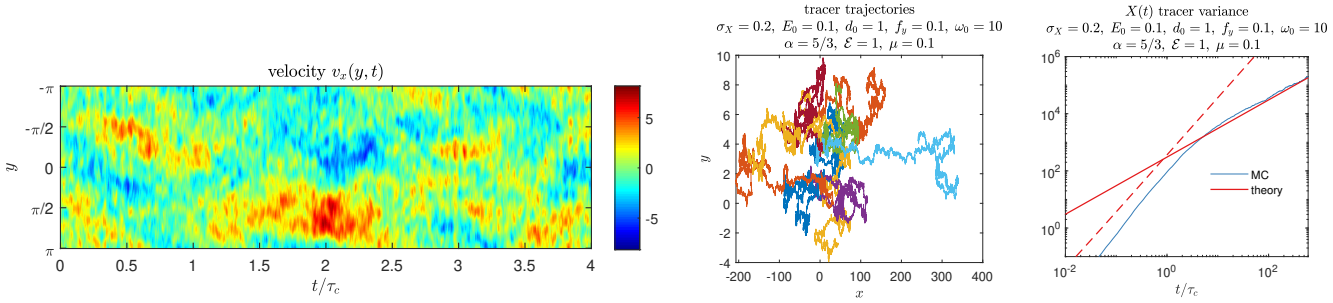


## 10 Conclusions

We proposed a stochastic turbulent shear model consisting of a randomly fluctuating mean and an aligned shear component to study passively advected Lagrangian particles. The proposed model is rich enough to highlight important differences in the Eulerian versus Lagrangian perspective that arise in more general flows. At the same time, the model is simple enough to admit exactly solvable statistics and thus serves as an important test problem for, e.g., Lagrangian data assimilation and parameter estimation algorithms. An important element of the turbulent shear model is that

it included a non-deterministic mean and a non-trivial shear term. We directly solved for both the Eulerian and Lagrangian statistics. We also derived theoretical predictions for the second-order moments for the Lagrangian particle trajectories. Then we compared and highlighted the differences between the Eulerian and Lagrangian perspective for this special model. We discussed how each model parameter affects Lagrangian particle advection and demonstrated accuracy of our derived formulae for the mixing rate with numerical comparisons. The numerical model regimes studies complemented the physical description of each model term, and demonstrated particle behavior and their extent in space and time. Future work utilizes the proposed model for combined filtering and parameter estimation of the turbulent Eulerian spectrum, which is a broadly important problem in atmospheric and ocean science and engineering.

***Acknowledgments***

A. J. M. acknowledges partial support by the Office of Naval Research through N00014-19-S-B001. M.A.M. is supported as a postdoctoral fellow on the same grant.

## References

1. Rossby, T. in *Lagrangian Analysis and Prediction of Coastal and Ocean Dynamics* (eds Griffa, A., Kirwan Jr., A. D., Mariano, A. J., Özgökmen, T. & Rossby, H. T.) 38–1 (Cambridge University Press, 2007).
2. Lumpkin, R. & Pazos, M. in *Lagrangian Analysis and Prediction of Coastal and Ocean Dynamics* (eds Griffa, A., Kirwan Jr., A. D., Mariano, A. J., Özgökmen, T. & Rossby, H. T.) 39–67 (Cambridge University Press, 2007).
3. Weil, J. C., Sykes, R. I. & Venkatram, A. Evaluating air-quality models: Review and outlook. *Journal of Applied Meteorology* **31,** 1121–1145 (1992).
4. Wang, Q. A. Probability distribution and entropy as a measure of uncertainty. *Journal of Physics A: Mathematical and Theoretical* **41,** 065004 (Jan. 2008).
5. Celis, C. & Figueira da Silva, L. F. Lagrangian mixing models for turbulent combustion: Review and prospects. *Flow, Turbulence and Combustion* **94,** 643–689 (Apr. 2015).
6. Holzner, M., Liberzon, A., Nikitin, N., Lüthi, B., Kinzelbach, W. & Tsinober, A. A Lagrangian investigation of the small-scale features of turbulent entrainment through particle tracking and direct numerical simulation. *Journal of Fluid Mechanics* **598,** 465–475 (2008).
7. Yeung, P. K. Lagrangian investigations of turbulence. *Annual Review of Fluid Mechanics* **34,** 115–142 (2002).
8. Pope, S. B. *Turbulent Flows* 1st ed. (Cambridge University Press, 2000).
9. Toschi, F. & Bodenschatz, E. Lagrangian properties of particles in turbulence. *Annual Review of Fluid Mechanics* **41,** 375–404 (2009).
10. Taylor, G. I. The spectrum of turbulence. *Proceedings of the Royal Society of London. Series A - Mathematical and Physical Sciences* **164,** 476–490 (1938).
11. Taylor, G. I. Diffusion by continuous movements. *Proceedings of the London Mathematical Society* **s2-20,** 196–212 (1922).
12. Batchelor, G. K. Diffusion in free turbulent shear flows. *Journal of Fluid Mechanics* **3,** 67–80 (1957).
13. Batchelor, G. K. The application of the similarity theory of turbulence to atmospheric diffusion. *Quarterly Journal of the Royal Meteorological Society* **76,** 133–146 (1950).
14. Richardson, L. F. Atmospheric diffusion shown on a distance-neighbour graph. *Proceedings of the Royal Society of London. Series A, Containing Papers of a Mathematical and Physical Character* **110,** 709–737 (Apr. 1926).
15. Bennett, A. F. A Lagrangian analysis of turbulent diffusion. *Reviews of Geophysics* **25,** 799–822 (1987).
16. Bennett, A. *Lagrangian Fluid Dynamics* (Cambridge University Press, 2006).
17. LaCasce, J. H. Statistics from Lagrangian observations. *Progress in Oceanography* **77,** 1–29 (2008).
18. Lilly, J. M., Sykulski, A. M., Early, J. J. & Olhede, S. C. Fractional Brownian motion, the Matérn process and stochastic modeling of turbulent dispersion. *Nonlinear Processes in Geophysics* **24,** 481–514 (2017).
19. Sawford, B. Turbulent relative dispersion. *Annual Review of Fluid Mechanics* **33,** 289–317 (2001).

20. Salazar, J. P. L. C. & Collins, L. R. Two-particle dispersion in isotropic turbulent flows. *Annual Review of Fluid Mechanics* **41,** 405–432 (2009).

21. Balwada, D., LaCasce, J. H. & Speer, K. G. Scale-dependent distribution of kinetic energy from surface drifters in the Gulf of Mexico. *Geophysical Research Letters* **43,** 10, 856–10, 863 (2016).

22. Beron-Vera, F. J. & LaCasce, J. H. Statistics of simulated and observed pair separations in the Gulf of Mexico. *Journal of Physical Oceanography* **46,** 2183–2199 (2016).

23. Roach, C. J., Balwada, D. & Speer, K. Global Observations of Horizontal Mixing from Argo Float and Surface Drifter Trajectories. *Journal of Geophysical Research: Oceans* **123,** 4560–4575 (2018).

24. Young, W. R., Rhines, P. B. & Garrett, C. J. R. Shear-flow dispersion, internal waves and horizontal mixing in the ocean. *Journal of Physical Oceanography* **12,** 515–527 (1982).

25. Majda, A. J. & Gershgorin, B. Elementary models for turbulent diffusion with complex physical features: eddy diffusivity, spectrum and intermittency. *Philosophical Transactions of the Royal Society A: Mathematical, Physical and Engineering Sciences* **371** (2013).

26. Majda, A. J. & Kramer, P. R. Simplified models for turbulent diffusion: Theory, numerical modelling, and physical phenomena. *Physics Reports* **314,** 237–574 (1999).

27. Majda, A. J. & Tong, X. T. Intermittency in turbulent diffusion models with a mean gradient. *Nonlinearity* **28,** 4171 (2015).

28. Qi, D. & Majda, A. J. Predicting fat-tailed intermittent probability distributions in passive scalar turbulence with imperfect models through empirical information theory. *Communications in Mathematical Sciences* **14,** 1687–1722 (2016).

29. Gershgorin, B. & Majda, A. J. Filtering a statistically exactly solvable test model for turbulent tracers from partial observations. *Journal of Computational Physics* **230,** 1602–1638 (2011).

30. Majda, A. J. & McLaughlin, R. M. The effect of mean flows on enhanced diffusivity in transport by incompressible periodic velocity fields. *Studies in Applied Mathematics* **89,** 245–279 (1993).

31. Mohamad, M. A., Cousins, W. & Sapsis, T. P. A probabilistic decomposition-synthesis method for the quantification of rare events due to internal instabilities. *Journal of Computational Physics* **322,** 288–308 (2016).

32. Chen, N. & Majda, A. J. Conditional Gaussian systems for multiscale nonlinear stochastic systems: Prediction, state estimation and uncertainty quantification. *Entropy* **20** (2018).

33. Liptser, R. S. & Shiryaev, A. N. *Statistics of Random Processes II. Applications* 2nd ed. *Stochastic Modelling and Applied Probability* **6** (Springer-Verlag Berlin Heidelberg, 2001).

34. Chen, N. & Majda, A. J. A new efficient parameter estimation algorithm for high-dimensional complex nonlinear turbulent dynamical systems with partial observations. *(submitted)* (2019).

35. Apte, A., Jones, C. K. R. T. & Stuart, A. M. A Bayesian approach to Lagrangian data assimilation. *Tellus A: Dynamic Meteorology and Oceanography* **60,** 336–347 (2008).

36. Molcard, A., Özgökmen, T. M., Griffa, A., Piterbarg, L. I. & Chin, T. M. in *Lagrangian Analysis and Prediction of Coastal and Ocean Dynamics* (eds Griffa, A., Kirwan Jr., A. D., Mariano, A. J., Özgökmen, T. & Rossby, H. T.) 172–203 (Cambridge University Press, 2007).

37. Kuznetsov, Y. A. *Elements of Applied Bifurcation Theory* 3rd ed. *Applied Mathematical Sciences* **112** (Springer-Verlag New York, 2004).

38. Kuznetsov, L., Ide, K. & Jones, C. K. R. T. A method for assimilation of Lagrangian data. *Monthly Weather Review* **131,** 2247–2260 (2003).

39. Chen, N. & Majda, A. J. Beating the curse of dimension with accurate statistics for the Fokker-Planck equation in complex turbulent systems. *Proceedings of the National Academy of Sciences* **114,** 12864–12869 (2017).

40. Mohamad, M. A. & Majda, A. J. Recovering the Eulerian energy spectrum from noisy Lagrangian tracers. *(submitted)* (2019).

41. Chen, N., Majda, A. J. & Tong, X. T. Noisy Lagrangian tracers for filtering random rotating compressible flows. *Journal of Nonlinear Science* **25,** 451–488 (June 2015).

42. Chen, N. & Majda, A. J. Model error in filtering random compressible flows utilizing noisy Lagrangian tracers. *Monthly Weather Review* **144,** 4037–4061 (2016).

43. Majda, A. J. & Harlim, J. *Filtering Complex Turbulent Systems* (Cambridge University Press, 2012).

44. Pavliotis, G. A. *Stochastic Processes and Applications. Diffusion Processes, the Fokker-Planck and Langevin Equations Texts in Applied Mathematics* **60** (Springer-Verlag New York, 2014).

## A Solution and statistical properties of the velocity model

The following results are standard and can also be found in references such as [43, 44].

### *A.1 Statistics of the spatially uniform background mean*

The analytical solution of the background velocity field

$$d\boldsymbol{w}(t) = \big((-\Gamma_0 + \Omega_0)\boldsymbol{w}(t) + \boldsymbol{f}_0\big)\,dt + \Sigma_0\,d\boldsymbol{W}_0(t), \tag{78}$$

may be solved by an integrating factor. With initial condition $\boldsymbol{w}(0) = \boldsymbol{w}_0 = (w_{0x}, w_{0y})$, define $A = -\Gamma_0 + \Omega_0$, then

$$\boldsymbol{w}(t) = e^{At}\boldsymbol{w}_0 + \int_0^t e^{A(t-s)}\boldsymbol{f}_0(s)\,ds + \int_0^t e^{A(t-s)}\Sigma_0\,d\boldsymbol{W}_0(s). \tag{79}$$

A simpler way to proceed is by adopting the complex variable approach. The dissipation matrix $\Gamma_0$, the skew symmetric rotation matrix $\Sigma_0$, and the diffusion matrix $\Sigma_0$ are explicitly

$$\Gamma_0 = \begin{pmatrix} d_0 & 0 \\ 0 & d_0 \end{pmatrix}, \quad \Omega_0 = \begin{pmatrix} 0 & -\omega_0 \\ \omega_0 & 0 \end{pmatrix}, \quad \Sigma_0 = \begin{pmatrix} \sigma_0 & 0 \\ 0 & \sigma_0 \end{pmatrix}. \tag{80}$$

These $2 \times 2$ matrices can be represented by complex numbers. Hence, we can represent the velocity $\boldsymbol{w} = (w_x, w_y)$ as a complex variable $w = w_x + iw_y$, satisfying

$$dw(t) = \big((-d_0 + i\omega_0)w(t) + f_0\big)dt + \sqrt{2}\sigma_0\,dW_0(t), \tag{81}$$

where $f_0 = f_{0x} + if_{0y}$, with $\boldsymbol{f}_0 = (f_{0x}, f_{0y})$. Define $p_0 = -d_0 + i\omega_0$, the solution of this complex Ornstein-Uhlenbeck process is given by

$$w(t) = e^{p_0 t}w_0 - \frac{f_0}{p_0}(1 - e^{pt}) + \sqrt{2}\sigma_0 \int_0^t e^{p_0(t-s)}\,dW(s), \tag{82}$$

where $w_0 = w_{0x} + iw_{0y}$. Assuming a constant initial condition, the mean and variance of this process are

$$\overline{w}(t) = e^{p_0 t}w_0 - \frac{f_0}{p_0}(1 - e^{p_0 t}) = -\frac{f_0}{p_0} + e^{p_0 t}\Big(w_0 + \frac{f_0}{p_0}\Big) \tag{83}$$

$$\mathrm{Var}(w(t)) = \frac{\sigma_0^2}{d_0}(1 - e^{-2d_0 t}), \tag{84}$$

hence asymptotically $w(t) \sim N(-\frac{f_0}{p_0}, \frac{\sigma_0^2}{d_0})$, or always if $w_0 \sim N(-\frac{f_0}{p_0}, \frac{\sigma_0^2}{d_0})$. Furthermore, the temporal autocorrelation function can also be shown to be

$$R_w(t, t') = \big\langle (w(t) - \overline{w}(t))(w(t') - \overline{w}(t'))^* \big\rangle = \frac{\sigma_0^2}{d_0} e^{d_0(t-t') - iw_0(t'-t)}(1 - e^{-2d_0 t}), \tag{85}$$

and in the asymptotic regime by,

$$R_w(\tau) = \frac{\sigma_0^2}{d_0} e^{(-d_0 - iw_0)\tau}. \tag{86}$$

### *A.2 Statistics of the modal coefficients of the shear term*

Each Fourier mode also satisfies a complex Ornstein-Uhlenbeck process and repeating the calculations from the previous section shows that the solution of

$$da_{\boldsymbol{k}}(t) = \big(p_{\boldsymbol{k}} a_{\boldsymbol{k}}(t) + f_{\boldsymbol{k}}\big)\,dt + \sigma_{\boldsymbol{k}}\,dW_{\boldsymbol{k}}(t), \tag{87}$$

where $p_{\boldsymbol{k}} = -d_{\boldsymbol{k}} + i\omega_{\boldsymbol{k}}$, with initial conditions $a_{\boldsymbol{k}}(0) = a_{\boldsymbol{k}0}$, is given by

$$a_{\boldsymbol{k}} = e^{p_{\boldsymbol{k}} t}a_{\boldsymbol{k}0} - \frac{f_{\boldsymbol{k}}}{p_{\boldsymbol{k}}}(1 - e^{p_{\boldsymbol{k}} t}) + \sigma_{\boldsymbol{k}} \int_0^t e^{p_{\boldsymbol{k}}(t-s)}\,dW(s), \tag{88}$$

with mean and variance, respectively,

$$\overline{a_{\boldsymbol{k}}}(t) = e^{p_{\boldsymbol{k}}t}a_{\boldsymbol{k}0} - \frac{f_{\boldsymbol{k}}}{p_{\boldsymbol{k}}}(1 - e^{p_{\boldsymbol{k}}t}) = -\frac{f_{\boldsymbol{k}}}{p_{\boldsymbol{k}}} + e^{p_{\boldsymbol{k}}t}\Big(a_{\boldsymbol{k}0} + \frac{f_{\boldsymbol{k}}}{p_{\boldsymbol{k}}}\Big) \tag{89}$$

$$\mathrm{Var}(a_{\boldsymbol{k}}(t)) = \frac{\sigma_{\boldsymbol{k}}^2}{2d_{\boldsymbol{k}}}(1 - e^{-2d_{\boldsymbol{k}}t}), \tag{90}$$

hence asymptotically $a_{\boldsymbol{k}} \sim N(-\frac{f_{\boldsymbol{k}}}{p_{\boldsymbol{k}}}, \frac{\sigma_{\boldsymbol{k}}^2}{2d_{\boldsymbol{k}}})$, or always if $a_{\boldsymbol{k}0} \sim N(-\frac{f_{\boldsymbol{k}}}{p_{\boldsymbol{k}}}, \frac{\sigma_{\boldsymbol{k}}^2}{2d_{\boldsymbol{k}}})$. The autocorrelation function in the asymptotic regime can be shown to be given by,

$$R_{a_{\boldsymbol{k}}}(\tau) = \frac{\sigma_{\boldsymbol{k}}^2}{2d_{\boldsymbol{k}}}e^{(-d_{\boldsymbol{k}} - i\omega_{\boldsymbol{k}})\tau}. \tag{91}$$